Fatigue life estimation of pre-corroded 42CrMo4 subjected to accelerated pitting corrosion method

Mario Álvarez[1,*], Miguel Muñiz-Calvente[2], Iker Urresti[1], Mikel Escalero[1], Javier Gracia[2]

[1]Structural Reliability Department, Mechanics Area, Ikerlan Technology Research Center, P J.M. Arizmendiarreta Ibilbidea, 2, 20500 Arrasate-Mondragón, Spain

[2]Department of Construction and Manufacturing Engineering, University of Oviedo, C\Pedro Puig Adam, s/n, 33204 Gijón, Spain

*e-mail address: maalvarez@ikerlan.es

Abstract

One of the main causes of failure of the components and structures used by Oil&Gas and offshore industries is associated to pitting corrosion. In this work, two main objectives have been defined. Firstly, the main variables to perform accelerated pitting corrosion on 42CrMo4 steel under laboratory conditions are defined. These accelerated corrosion tests have been performed to obtain pitting defects as similar as possible to the real ones observed in offshore environments. Secondly, fracture mechanics has been applied to predict the fatigue propagation of pitting defects until the final fracture, and a sensitivity analysis has been performed to determine the influence of geometric parameters on the fatigue failure predictions. Finally, a series of fatigue tests were carried out to obtain the S-N curves of the pre-corroded steel specimens and the results have been compared with the fatigue predictions. The main conclusion of the paper is that fracture mechanic approaches can be used to predict the fatigue life of 42CrMo4 subjected to corrosive environments in a reasonably conservative way.

Keywords

Pitting, accelerated corrosion, fatigue, life estimation, sensitivity analysis.

1. Introduction

Components in corrosive environments are very susceptible to pitting corrosion. This type of localized corrosion represents an important source of surface degradation, which reduces the fatigue life of the material and can lead to the catastrophic failure of the structure [1]. Structural materials in sectors, such as Oil&Gas and offshore industries, are subject to very aggressive environments [2][3] that can reduce the fatigue life of the material and structures significantly for corrosion-induced surface defects [4][5] . The

deposition of sodium chloride and other substances dissolved in seawater generate pitting that can be considered as surface defects or fatigue crack initiators [4][7][8].

With the aim of characterizing the fatigue behavior of corroded components, it is necessary to obtain corroded samples with pitting defects as similar as possible to the real ones registered in real conditions. Nevertheless, this would imply the natural exposure of samples to the real corrosive environment during a very large period, which is too expensive and almost impossible. For that reason, it is necessary to define accelerated tests under laboratory conditions to produce a corrosive environment able to generate pitting defects analogous to the ones observed on real corrosion processes [9][10]. This accelerated laboratory-based test are commonly based on the immersion of metallic samples on a ferric chloride solution based on the guidelines of the ASTM G48 [11]. However, several parameters related to the laboratory-based test, such as the water purity, pH, duration and temperature of testing, are not properly defined on ASTM G48 [12]. For this reason, the first objective of this paper is to define the parameters involved in accelerated corrosion tests related to the generation of pitting defects, like those found in 42CrMo4 samples in service. This material has been selected because it is extensive used in mechanical engineering and vehicles construction (gears, transmission parts, crankshafts, cranks, etc.).

Localized pre-corrosion defects increase the risk of fatigue crack initiation and propagation due to the increment of stress concentration around pits [8],[13],[14]. In this work, pre-corroded samples have been tested under fatigue conditions to determine the reduction of fatigue life associated to pitting defects. Thereafter, the fatigue lifetimes observed experimentally has been compared to predictions failure based on fracture mechanics approaches. Pitting defects have been assumed as surface cracks and the range of the stress intensity factor (ΔK) has been used to predict crack growth rates by the Paris Law [15] and the NASGRO equation [16]. Different parameters influenced those predictions, such as the parameters of the crack growth law associated to the material or the pit geometry. Consequently, a sensitivity analysis to the material parameters and main pit geometry factors (crack center offset and aspect ratio) has been performed.

This paper is organized as follows. Firstly, the accelerated corrosion tests employed to generate pitting defects on the samples surfaces are described. Then, the experimental results obtained from the fatigue testing of the pre-corroded specimens are analyzed and compared with fatigue predictions based on fracture mechanics. After that, a sensitivity analysis of the material and geometric variables involved on the fatigue predictions are analyzed. Finally, the mean results and conclusions of the paper are summarized.

2. Accelerated corrosion tests

2.1 Material

The material used in this investigation was the high strength low-alloy 42CrMo4, which is characterized by the following chemical composition: 0,38-0,45 %C; 0,9-1,2 % Cr; 0,15-0,3 % Mo; 0,17-0,37 % Si; 0,5-0,8 % Mn; 0,035%S; and balance Fe. This material has been selected for its widely use on applications related to mechanical engineering and vehicles construction, such as gears, transmission parts, crankshafts and cranks.

Regarding the basic material properties, the 42CrMo4 quenched and tempered steel is characterized by a Young modulus equal to 220 GPa, a Poisson ratio equal to 0.3, Rockwell hardness 25 HRC, and a flow strength (σ_0) of 749 MPa, which have been characterized according to UNE-EN ISO 6892-1:2010 [17] as reported in [18]. The flow strength is the average between the yield and ultimate tensile strengths.

2.2 Geometry

Dog-bone specimens dimensioned according to ISO 1099 [19] (See Figure 1) have been machined to perform the accelerated corrosion tests. Mechanical grinding with Silicon Carbide (SiC) papers was used to polish the surfaces until a mirror finish was reached. The geometry was selected to satisfy the necessary conditions to perform a fatigue experimental campaign on a servo-hydraulic machine, with the aim of characterizing the reduction of fatigue life due to the induced pitting corrosion.

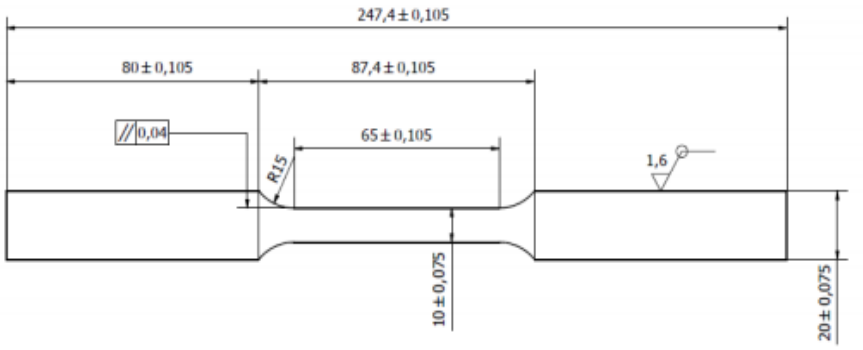

Figure 1. Geometry of the samples subjected to accelerated corrosion and fatigue tests

2.3 Test conditions

The pitting corrosion resistance of 42CrMo4 steel was determined according to ASTM G48 method A (ferric chloride pitting test) [20]. Despite ferric chloride solution is considered a very aggressive medium, the corrosion pits obtained under this solution are similar to the ones obtained under real seawater conditions [12].

In this study, 100g of reagent grade ferric chloride FeCl3.6H2O was dissolved in 900 ml of Type IV reagent water. The ratio of solution volume to specimen surface area was at least 5 ml/cm^2. A temperature of 22 ± 2ºC was used, according to standard recommendations.

Regarding test duration, two immersion times were evaluated to compare the pitting characteristics obtained. On the one hand, an immersion time of 72 hours was defined accordingly to the suggestions of the ASTM G48 [20]. On the other hand, an immersion time of 140 hours was proposed to reach deeper pits, which could conduct to higher reductions of fatigue life. In both cases, once the immersion time was completed, the specimens were rinsed with water and scrubbed with a nylon brush under running water to remove corrosion products attached to the surface.

As observed in literature [21], after the immersion of the samples into the static corrosive solution, hydrogen bubbles were produced (see Figure 2) and the solution above the sample progressively saturates with hydrogen. Thus, the oxygen level above the samples could be reduced by the hydrogen displacement. To reduce that effect and guarantee that the area of interest is completely surrounded by the corrosive medium, the samples were placed in flat surface orientation and elevated from the bottom of the container by means of PVC supports located on both ends, so there was not direct contact between the specimen and the bottom of the container.

Figure 2. Formation of hydrogen bubbles after immersion in ferric chloride solution

2.4 Results and discussion

After the first accelerated corrosion test (72 h) was completed, the surfaces of the samples were analyzed by a FEI Quanta 200 scanning electron microscope. As can be observed on Figure 3, pit width was in the range of 30-100 µm (with numerous pits around 45-65 µm wide), and the pit depth ranges from 17 to 19 µm.

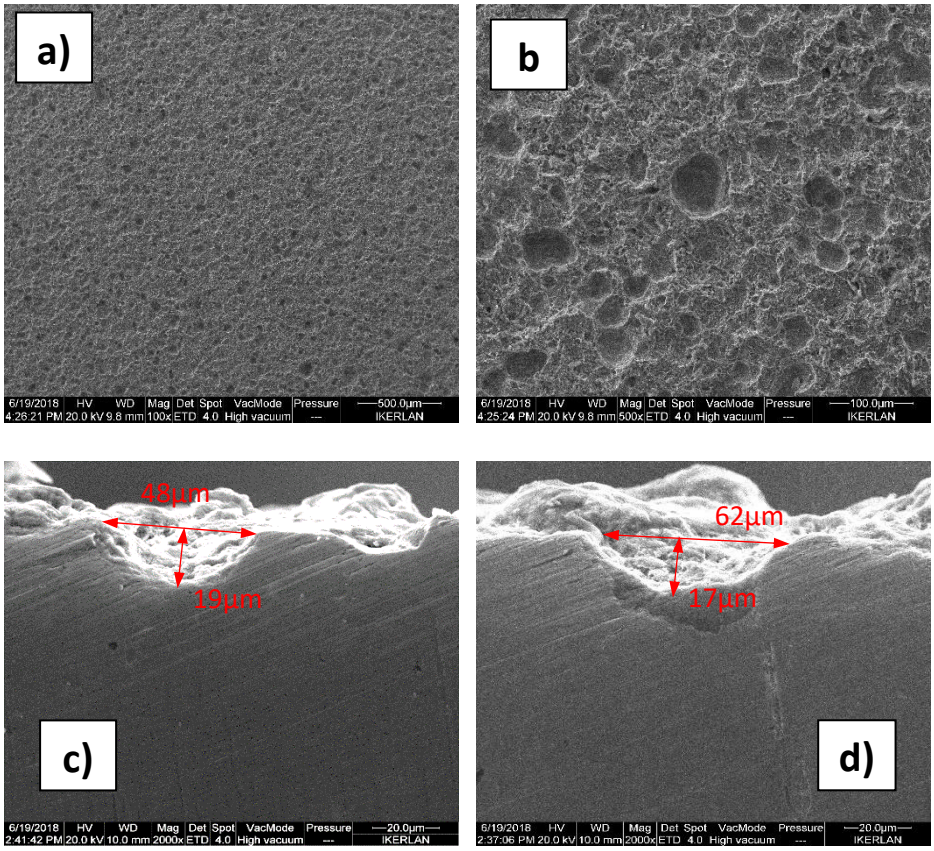

Figure 3. Pits generated in fatigue sample after 72h accelerated corrosion test: a) Surface 100X; b) Surface 500X; c) and d) width and depth of two representative pits.

Taking into account that pit depth observed in real cases of steel pitting corrosion is greater than 20 µm [22], the results obtained after 72h accelerated corrosion test did not represent surface damages comparable to a real case study. For that reason, this samples were disregarded as candidates to characterize the fatigue behavior of real damage components. The samples exposed to the corrosive solution during 140 h shown external surface damages more similar to the ones find on real cases, observing pit depth greater than 20 µm as intended (Figure 4). Figure 5 shows the surface appearance of 4 different dog-bone shaped samples pre-corroded during 140 h, and Table 1 summarizes the maximum width of the pits observed on these samples.

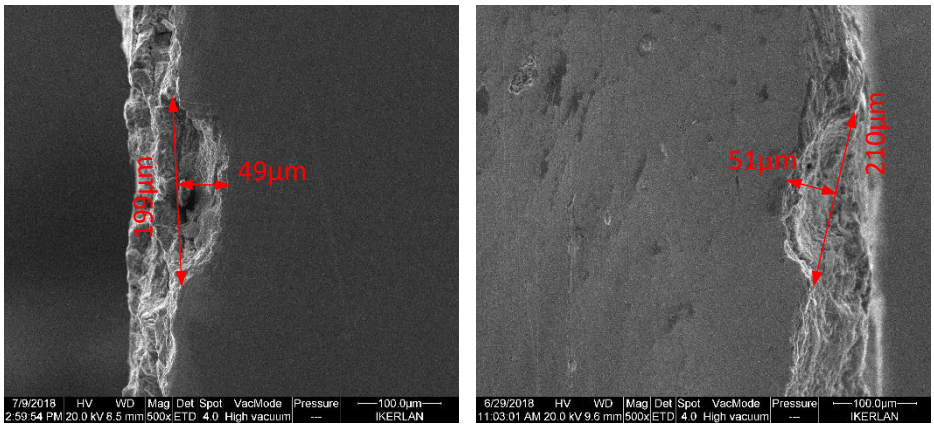

Figure 4. Pits generated in fatigue sample after 140h accelerated corrosion test: width and depth of two representative pits

Sample	Maximum Pit width (µm)
Sample1	298
Sample2	248
Sample3	250
Sample4	244

Table 1. Maximum pit width of 140 h pre-corroded samples measured in SEM images

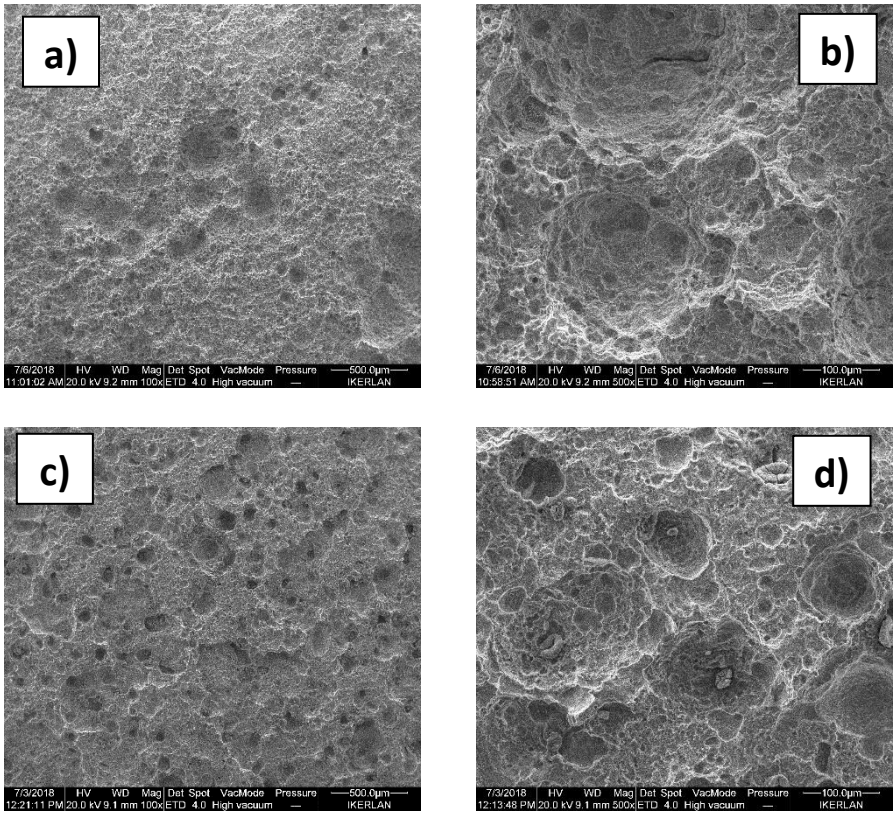

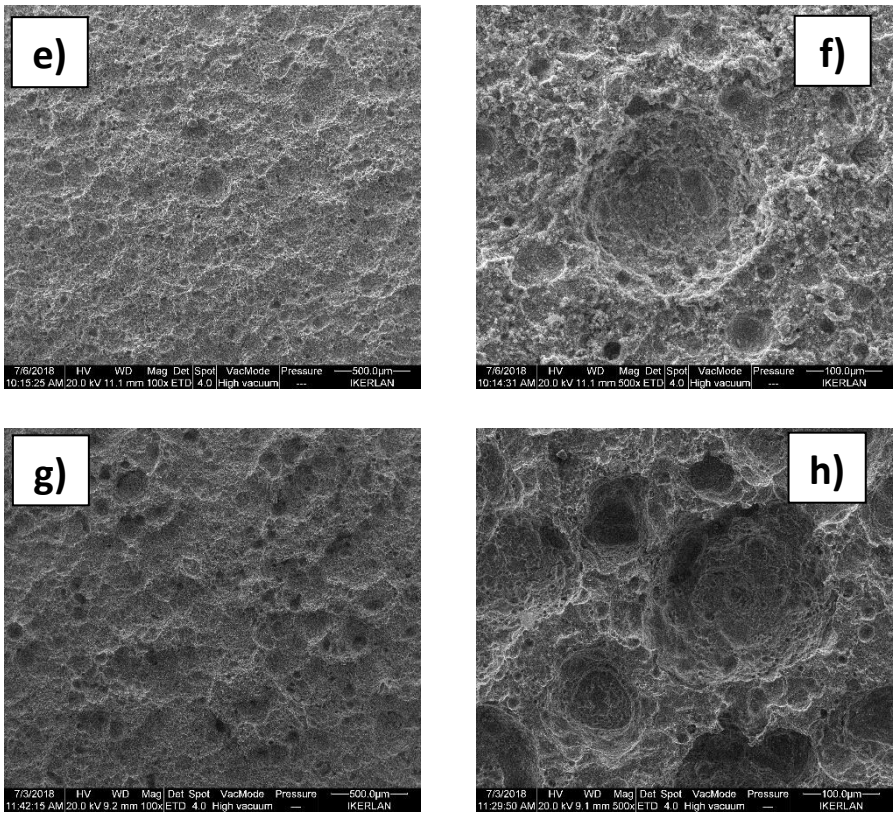

Figure 5. Surface corrosion appearance of fatigue samples after 140h immersion time: a) Sample1-100X, b) Sample1-500X, c) Sample2-100X, d) Sample2-500X, e) Sample3-100X, f) Sample3-500X, g) Sample4-100X, and h) Sample4-500X.

After completion of this part of the study, it was verified that ferric chloride solution generated pitting corrosion on 42CrMo4 surface, observing a semi-elliptical pit shape. However, it was necessary to increase the recommended 72 h test duration in ASTM G48 in order to generate pitting depth greater than 20 µm. Although the ratio of solution volume to specimen surface area was at least 5 ml/cm^2 and a temperature of 22 ± 2ºC was used, according to standard recommendations, it is important to remark that factors such aeration or pH monitoring could be considered in future in order to optimize the pitting process, as suggested in [21].

3. Fatigue testing of pre-corroded samples

3.1 Test conditions

After finishing the accelerated corrosion test explained in the previous section, the corroded specimens obtained have been tested under uniaxial fatigue conditions in order to characterize their fatigue life. Fatigue tests were carried out on a servo-hydraulic testing machine (SERVOSIS ME-401/15) under a stress ratio of R = 0.1 and a frequency of 10 Hz. The maximum stress level applied was in the range between 60-90% σ_y.

3.2 Results and discussion

The results obtained from the experimental campaign can be seen on Table 2 and Figure 6. Experimental results were evaluated by ProFatigue software [23] in order to obtain the probabilistic fatigue field (p-S-N) of the corroded samples. The probabilistic fatigue field obtained was compared to the probabilistic field of undamaged 42CrMo4 material [24]. The endurance limit was obtained by the Castillo and Cantelli model [25] for both, damaged and undamaged conditions (see Figure 6). As can be observed onFigure 6, the probabilistic fatigue fields observed for the undamaged and the damage material are significantly different, so the differences registered cannot be attributable to the inherent scatter of the material but the corrosion damage process. Furthermore, all fatigue tests were performed below the endurance fatigue limit of undamaged 42CrMo4 material[24], thus, failures must be related to initial damages presented on the surface of the specimens (pit defects). Although these defects are not as sharp as a fatigue propagating crack, the assumption of surface defects as fatigue cracks should be a conservative approach that could conduct to reliable fatigue failure predictions of corroded components.

Sample Number	$\%\sigma_y$	Stress Range Δσ (MPa)	Experimental fatigue life (cycles)	Estimated fatigue life (cycles)
1	60	349.2	1,240,912	499,201
2	70	407.7	1,120,593	275,033
3	75	436.5	135,471	228,340
4	80	466.2	233,147	139,235
5	85	495	164,501	88,069
6	87	506.7	113,150	94,743
7	90	523.8	75,473	119,807

Table 2. Experimental fatigue lives of pre-corroded 42CrMo4 samples with R=0.1

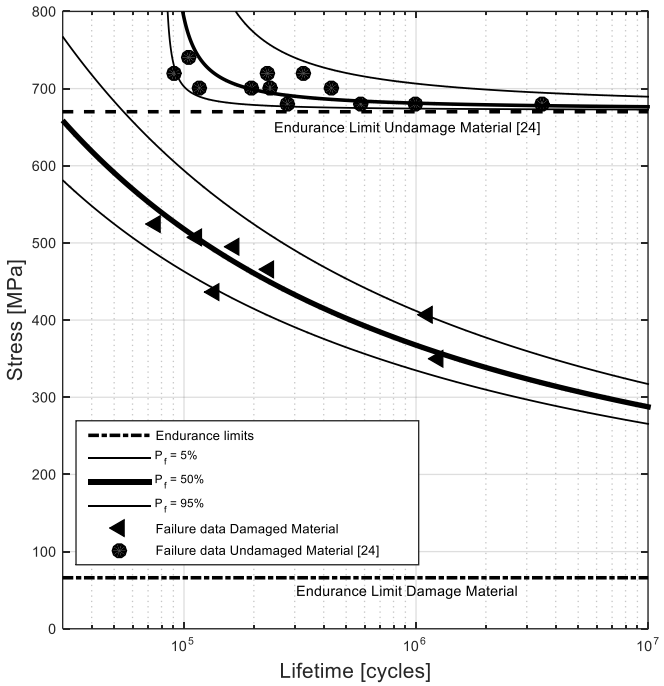

Figure 6. Failure probability curves at 0%, 5%, 50% and 95% obtained with ProFatigue software for corroded and non-corroded 42CrMo4.

4. Fatigue life prediction of pre-corroded samples based on fracture mechanics

4.1 Geometric characterization of pit defects

Once all specimens were broken by fatigue testing, detailed fractographic analysis was performed by a scanning electron microscope (SEM) to examine the fracture surface and surface area. Post-fracture fractography was used to locate and measure the width and depth of the pit that originates the fatigue crack growth and, therefore, the final fatigue failure. Figure 7 shows SEM images of the fatigue and fracture surfaces of the specimens. After fatigue failure, crack origin zone was located through macroscopic observation. This zone was microscopically observed with more detail in order to identify the dominant crack-nucleating pit by detecting the presence of surface ripples, known as striations, on the fatigue fracture surface [26] [27]. In each specimen, the point related to the dominant crack-nucleating pit has been marked by a red arrow.

According to the pit shapes observed (Figure 7), these were considered as semi-elliptical surface crack defects (Figure 8). Once the main critical pits were identified, the main dimensions of each of them to be characterized as a semi-elliptical surface crack were measured (Table 3): depth (a), width ($2c$) and position (Crack center offset, (B)). According to the values shown in Table 3, corroded samples have an average

ratio $2c/a \approx 3.375$, which is in agreement with the defects reported in [28] for steel samples subjected to seawater corrosion ($2 < 2c/a < 5$).

195

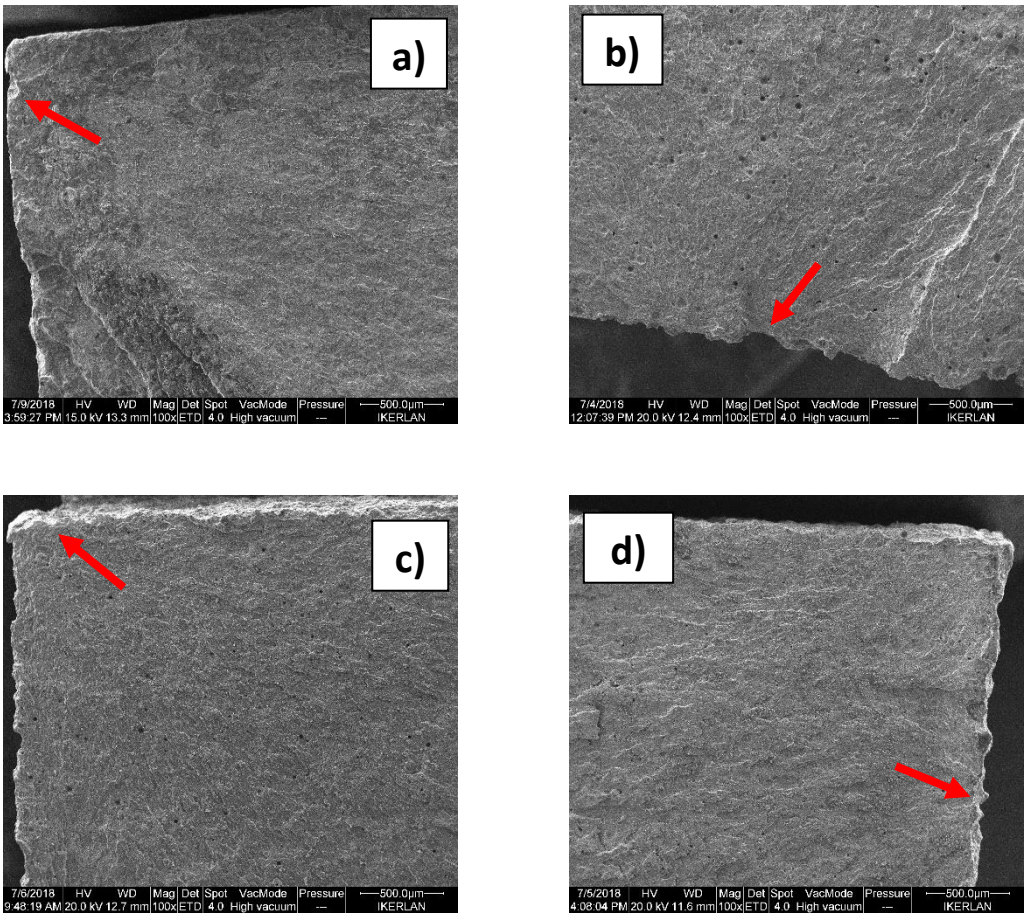

Figure 7. Fracture Surface analysis of fatigue specimens subjected to different stress levels: a) 70%σy, b) 75%σy, c) 85%σy, and d) 90%σy. Pits responsible for fatigue crack nucleation pointed with red arrows.

Sample Number	Pit depth *a* (µm)	Pit width *2c* (µm)	Crack center offset *B* (µm)	Initial *a/c*
1	48	201	350	0.478
2	64	191	300	0.670
3	65	281	910	0.463
4	51	309	219	0.330
5	127	390	435	0.651
6	86	299	230	0.575
7	119	220	1078	1.082

Table 3. Geometrical parameters of critical pits

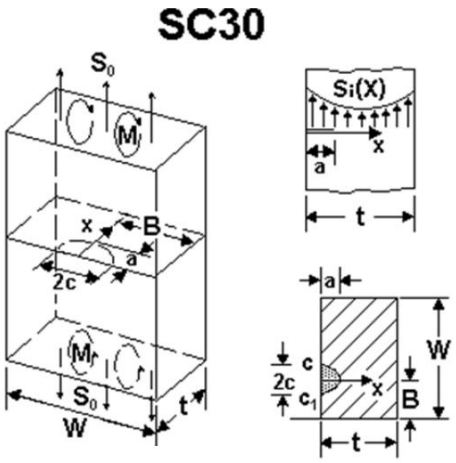

Figure 8. Semi-elliptical surface crack defects according to SC30 in NASFLA-NASGRO 8.1 [16]

4.2 Fatigue life estimation approach

In this study, fatigue crack growth was estimated by the analytical approach defined by the NASGRO equation:

$$\frac{da}{dN} = C\left[\frac{1-f}{1-R}\Delta K\right]^{n}\frac{\left(1-\frac{\Delta K_{th}}{\Delta K}\right)^{p}}{\left(1-\frac{K_{max}}{K_c}\right)^{q}} \qquad (1)$$

Where *da/dN* is the crack growth rate, *ΔK* is the applied stress-intensity factor range, and *R* is the stress ratio, ΔK_{th} is the fatigue threshold, K_{max} is the stress-intensity factor corresponding to peak applied load, and K_c is the critical stress intensity; *p* and *q* control the shape of the asymptotes in the threshold and critical growth regions, respectively; *f* is Newman's crack opening function. Besides, *C*, *n*, *p* and *q* are fitting coefficients considered as material properties and can be obtained by standardized experimental tests (ASTM E647-15 [29]).

The evolution of the stress intensity factor has been estimated by the NASGRO software taking into account the geometrical parameters included in Table 3. Finally, the Failure Assessment Diagram (FAD) [30] has been used to determine if the critical crack length has been reached, which conducts the final fracture of the sample.

FAD is a graph of the failure envelope of a cracked structure, expressed in terms of the two parameters *Kr* and *Lr* defined as follows:

- Ratio of the applied stress intensity factor to the appropriate material fracture toughness value (such as Kc or KIe)

$$K_r = K_{app}/K_{mat} \quad (3)$$

- Ratio of the total applied load contributing to the primary stresses to the plastic limit load of the cracked structure

$$L_r = P/P_L \quad (4)$$

The failure envelope is called the Failure Assessment Line (FAL). For the approaches currently included in NASGRO, the FAL is dependent only on the tensile properties of the material through the relationship *Kr = f(Lr)*. The FAL incorporates a cut-off at *Lr = Lrmax*, which defines the plastic collapse limit of the structure.

To use the FAD approach, assessment points with coordinates (K_r, L_r) calculated based on the applicable loads, crack type and crack size, and material properties are compared with the FAL. Assessment points that lie inside the envelope defined by the FAL indicate non-failure, while assessment points that lie outside the FAL indicate failure. For many fatigue crack growth analyses, the assessment points will initially be far inside the FAL envelope and will gradually grow towards the FAL envelope as the crack grows sub-critically.

4.3 Results and discussion

Following the procedure described above, the final fatigue life of each specimen was estimated. To do that, the crack growth parameters characterized previously by the authors for 42CrMo4 [18][30] were used. The same supplier of the material was selected, in order to reduce the uncertainty. Furthermore, the geometrical parameters measured for each critical pit were used to predict the fatigue crack growth.

Figure 9 shows the comparison between the predicted and experimental fatigue lives. As can be seen, fatigue life predictions based on NASGRO equation (Eq. (1)) are conservative in all cases, except for the two ones related to the higher fatigue loads (near the yield limit), which are not conservative but lie between the two bounds related to the assumable fatigue scatter. The degree of conservatism of the prediction is inversely proportional to the remote load level, the lower the remote load the higher the conservativism. This can be explained by the assumption of the pit defects as propagating cracks. In the case of undamaged 12% Cr stainless steels [32[32], fatigue life is manly dominated by the crack initiation process (nucleation). However, the corrosion effect impacts on fatigue life by reducing the necessary time to create a crack able to be propagated [14][33[33][34[34]. In this paper, the portion of the fatigue life related to crack initiation process (nucleation) has been disregarded, which implies a higher level of conservatism for lower remote stresses because the time to initiate a crack should be higher than for higher remote stresses. In any case,

it is important to remark that NASGRO predictions were generally conservative, which is desirable for fatigue life analysis of real structures in order to take Run/Repair/Replace decisions in a safely way.

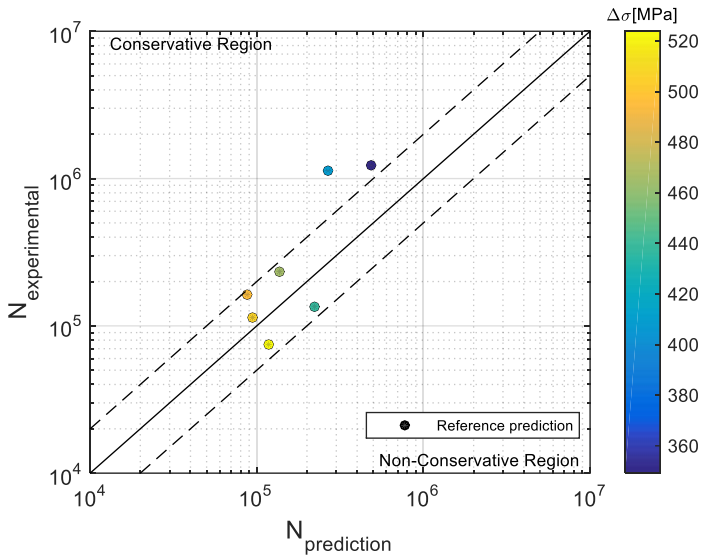

Figure 9. Comparison between experimental and predicted fatigue life

5. Sensitivity analysis

The predictions of fatigue life shown on the previous section aims to be the most reliable ones by using the NASGRO approach, because all uncertainties related to material properties and geometry factors influencing Eq. (1) have been mitigated. Nevertheless, the fatigue crack growth characterization of the material provided for the same supplier are not always available, so engineers and designers are commonly forced to use parameters available in literature, handbooks or standards/guidelines. Furthermore, the data related to the geometric characterization of the defects would not be available in a real case study, because the component would be corroded but not broken, so the pit depth (a) and width ($2c$) could not be measured directly by SEM, as has been done in this work. For that reason, and with the aim of quantifying the influence of both material and geometrical parameters on the fatigue prediction, a sensitivity analysis was performed.

5.1 Material properties

Firstly, the influence of fatigue crack growth parameters (C, n, p, q) has been studied. To do that, three additional sets of 42CrMo4 parameters (Table 4) obtained from the literature have been considered [16][35[35][36[36]. Regarding geometric parameters, the same pit geometry dimensions characterized by SEM (Table 3) were used in this study. As can be seen on Figure 10, the material parameters have a high influence on the final fatigue life predictions. As expected, the most conservative predictions were obtained

when using the curve fits for AISI 4140 in NASGRO material database, because these crack propagation curves are generated by conservative material parameters and safety factors. Analytical crack propagation simulation software and standards aim to provide conservative estimations that ensure compliance of the acceptance criteria.

Fatigue crack Growth Coefficients	*C*	*n*	*p*	*q*
Sander [35*[35]*]	$4.5 \cdot 10^{-11}$	2.2	0.8	0.5
Lebahn [36[36]	$1.8 \cdot 10^{-11}$	2.3	1.0	0.7
NASGRO database AISI 4140 [16]	$1.427 \cdot 10^{-11}$	2.5	0.5	0.5

Table 4. Example of crack growth parameters for 42CrMo4 available in the literature

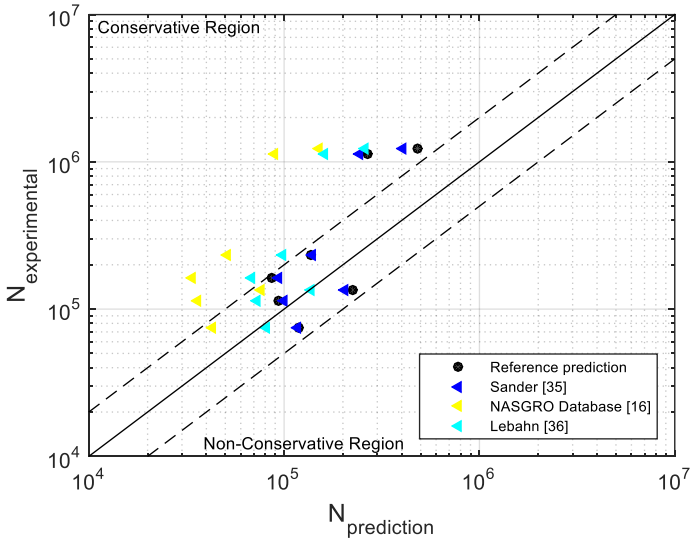

Figure 10. Results of the sensitivity analysis to material properties.

5.2 Influence of geometry factors: width and depth

In order to evaluate the impact of the geometry factors on the fatigue life, a sensitivity analysis varying the width (*c*) and depth (*a*) of pit corrosion defects has been performed. In order to analyze the influence of each parameter on the *a/c* ratio, pit width and depth were studied separately.

On the one hand, seven different pit depths were selected *a*={0.034; 0.068; 0.080; 0.135; 0.270; 0.540; 1.08} mm and the width (*c*) and crack center offset (*B*) were kept constant using the average values obtained by SEM , 0.135 mm 0.503mm respectively. This conducts to the following aspect ratios *a/c* = {0.250; 0.500; 0.592; 1.000; 2.000; 4.000; 8.000}.

Figure 11 shows that the results obtained in this sensitivity analysis. As can be expected, for a fixed width and center offset, the results shown that the higher the depth the lower the fatigue life. This implies that the increment in pit depth leads to a lifetime reduction (Figure 12), observing a lower number of cycles when the pit geometry changes from shallow to deep shape, which is in agreement with results previously published on the literature [8][37[37]. The observed fatigue life reduction could be associated to the

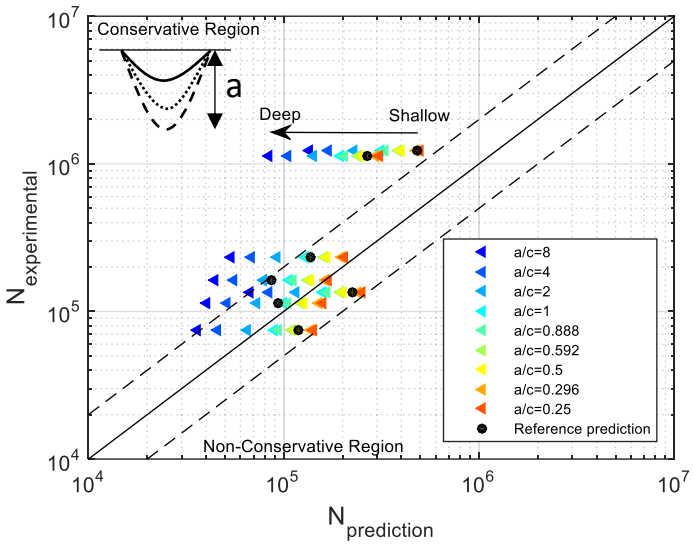

increment of the SIF value, which is related to the increment of pit depth [38].

Figure 11. Effect of aspect ratio on fatigue life. Influence of pit depth in the range 0.25-8 mm

Taking into account the results obtained for the mean value of a/c ratio obtained experimentally by SEM (a/c = 0.592), an error on the crack depth estimation could conduct to errors on fatigue crack growth around 19% reduction and 30% increment in the case of overestimating the crack depth on a 169% (a/c=1) or underestimate the crack depth on a 42% (a/c=0.25), respectively. *Figure 11* shows overestimation of crack depths until 1351% (a/c=8) with the aim of quantifying the errors obtained in the case of a very conservative approach, which could be interesting in the case of critical structures of components.

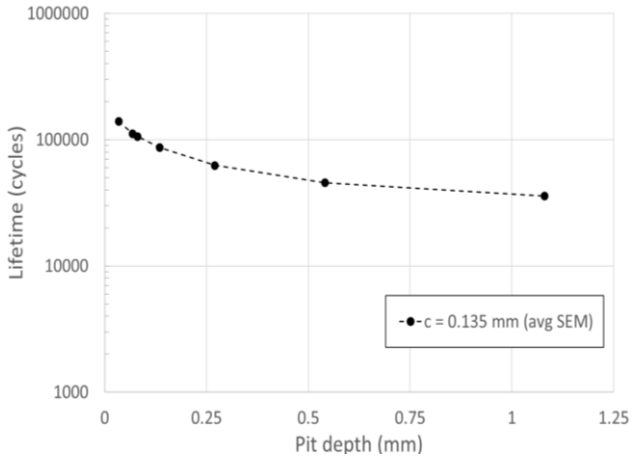

Figure 12. Relationship between lifetime and pit depth (load 90%σy)

On the one hand, seven different pit widths were selected *c*={0.320; 0.160; 0.135; 0.080; 0.040; 0.020; 0.010} mm and the depth (*a*) and crack center offset (*B*) were kept constant using the average values obtained by SEM, 0.08 mm 0.503mm respectively. This conducts to the same aspect ratios used on the previous sensitivity analysis, *a/c* = {0.250; 0.500; 0.592; 1.000; 2.000; 4.000; 8.000}.

Figure 13 depicts that for a fixed depth the narrowest crack would conduct to a largest fatigue life prediction. In this case, higher variations have been observed in terms of fatigue life predictions, and the underestimation of crack width could conduct to non-conservative results. As an example, an underestimation of crack width equal to 337% could conduct to a change of fatigue life prediction of around 60% increment (change from *a/c*=0.592 to *a/c*=2). In the case of overestimating the pit width, the fatigue predictions will be more conservative.

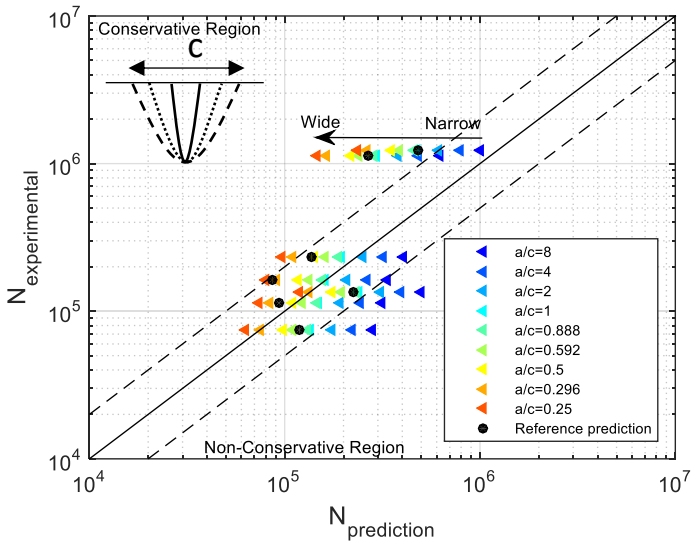

Figure 13. Effect of aspect ratio on fatigue life. Influence of pit width in the range 0.01-0.32 mm

5.3 Position: crack center offset

Finally, the influence of pit location along sample width was analyzed, considering three different crack center offsets *B*= {0.197; 0.503; 3.9} mm, corresponding to near-corner, average position registered experimentally and centered on the sample, respectively. The rest of the parameters were fixed to the average values registered experimentally: *a*= 0.08 mm, *c*=0.135mm

According to Figure 14, fatigue life reduction is observed when pit location moves from the center towards the corner of the sample. S-N curves show that fatigue life reduction is more significant as the pit location is closer to the corner.

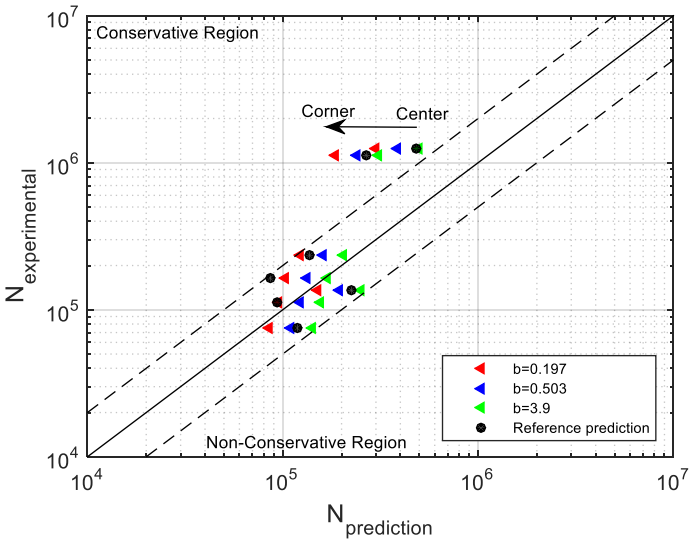

Figure 14. Crack center offset effect on fatigue life

6. Conclusions

According to the results obtained from the accelerated corrosion tests and the fatigue analysis, the following conclusions can be stated:

- Following ASTM G48 method, the corrosion pits obtained with 42CrMo4 steel were similar to the ones obtained under real seawater conditions.
- A fracture mechanics approach, based on the NASGRO equation and the assumption of corrosion pit defects as semi-elliptical surface cracks, can be considered to predict fatigue life of corroded components in a conservative way.
- According to the sensitivity analysis, it is recommended to characterize the fatigue crack growth law for the exact corroded material under study (same supplier), because the use of values provided by standards, guidelines or literature could conduct to very conservative predictions..
- The overestimation of pit depth or width conduct to a reduction of the predicted fatigue life.
- Concerning crack center offset parameter, fatigue life predictions showed that a more significant reductions as the pit location is closer to the corner.
- Aspect ratio *a/c* represents a geometrical parameter to be considered when assuming semi-elliptical pits, since lifetime increment was observed as the pit morphology changed from deep to shallow configuration.

References

[1] Jakubowski, M.; "Influence of Pitting Corrosion on Fatigue and Corrosion Fatigue of Ship and Offshore Structures, Part II: Load - Pit - Crack Interaction"; Polish Maritime Research 3 (87); Vol. 22; 2015; 57-66.

[2] Price J., Figueira R.B.; "Corrosion protection Systems and fatigue corrosion in offshore Wind Structures: current statuts and future perspectives"; Coatings 7 (25); 2017.

*[3] Iannuzzi, M., Barnoush, A., Johnsen, R.; "Materials and corrosion trends in offshore and subsea oil and gas production"; npj Mater Degrad **1,** 2; 2017.*

[4] Guo T., Liu Z., Correia J., de Jesus A.; "Experimental study on fretting-fatigue of bridge cable wires"; International Journal of Fatigue; Volume 131, 2020.

[5] Liu Z., Guo T., Yu X., Huang X., Correia J.; "Corrosion fatigue and electrochemical behaviour of steel wires used in bridge cables"; Fatigue Fract Eng Mater Struc 44; 2021; 63-73.

[6] Kondo Y.; "Prediction of fatigue crack growth initiation life based on pit growth"; Corrosion Science; Vol. 45; No. 1; 1989; 7-11.

[7] Rokhlin S.I., Kim J.Y, Nagy H., Zoofan B.; "Effect of pitting corossion on fatigue crack initiation and fatigue life"; Engineering Fracture Mechanics 62; 1999; 425-444.

[8] Dolley E.J., Lee B., Wei R.P.; "The effect of pitting corrosion on fatigue life"; Fatigue Fract Eng Mater Struct 23(7); 2000; 555–560

[9] Degerbeck J.; "On accelerated pitting and crevice corrosion tests"; Journal of the Electrochemical Society; Vol. 20; No. 2; 1973; 175-182.

[10] Oldfield J.W.; "Test techniques for pitting and crevice corrosion resistance of stainless steels and nickel-base alloys in chloride-containing environments"; International Materials Review; Vol. 32; No. 3; 1987; 153-172.

[11] ASTM G48-03; "Standard Test Methods for Pitting and Crevice Corrosion Resistance of Stainless Steels and Related Alloys by Use of Ferric Chloride Solution"; Philadelphia, Pa.; American Society for Testing Materials.

[12] Corbett R.A.; "Problems utilizing ASTM G48 to evaluate high-alloy stainless steels", Corrosion 92 Conference; NACE; 1992; paper 298.

[13] Walde K., Brockenbrough J.R., Craig B.A., Hillberry B.M.; "Multiple fatigue crack growth in pre-corroded 2024-T3 aluminum"; International Journal of Fatigue 27; 2005; 1509-1518.

[14] Kermanidis A.T., Petroyiannis P.V., Pantelakis S.G.; "Fatigue and damage tolerance behaviour of corroded 2024 T351 aircraft aluminum alloy"; Theoretical and Applied Fracture Mechanics 43; 2005; 121-132.

[15] Paris P.C., Erdogan F.A.; "A critical analysis of crack propagation laws"; Transactions of ASME Journal of Basic Engineering; 1963; 528-534.

[16] NASGRO; Fracture Mechanics and Fatigue Crack Growth Analysis Software; 2016.

[17] UNE-EN ISO 6892-1:2010, Metallic materials - Tensile testing - Part 1: Method of test at room temperature

[18] Escalero M., Muniz-Calvente M., Zabala H., Urresti I.; "Suitability of constraint and closure models for predicting crack growth in generic configurations"; Engineering Fracture Mechanics, Volume 225, 2020.

[19] ISO 1099:2017(E); 3rd. ed.; 2017.

[20] ASTM G48-03; Standard Test Methods for Pitting and Crevice Corrosion Resistance of Stainless Steels and Related Alloys by Use of Ferric Chloride Solution; ASTM International; West Conshohocken, PA; 2003.

[21] Bhandari J., Lau S., Abbassi R., Garaniya V., Ojeda R., Lisson D., Khan F.; "Accelerated pitting corrosion test of 304 stainless steel using ASTM G48; experimental investigation and concomitant challenges"; Journal of Loss Prevention in the Process Industries; 2017.

[22] Zhang Y., Zheng K., Heng J., Zhu J.; "Corrosion-Fatigue Evaluation of Uncoated Weathering Steel Bridges"; Appl. Sci.; 9; 2019; 3461.

[23] Fernandez-Canteli A., Przbylla C., Nogal M., LopezAenlle M., Castillo E.; "ProFatigue: A software program for probabilistic assessment of experimental fatigue data sets"; Procedia Engineering 74; 2014; 236–241.

[24] Benedetti M., Santus C.; "Mean stress and plasticity effect prediction on notch fatigue and crack growth threshold, combining the theory of critical distances and multiaxial fatigue criteria"; Fatigue Fract Eng Mater Struct; 2018; 1-19

[25] Castillo E., Fernández-Cantelli A.; "A unified methodology for modeling fatigue damage", Springer, 2009.

[26] Murashkin M., Sabirov I., Prosvirnin D., Ovid'ko I., Terentiev V., Valiev R., Dobatkin S.; "Fatigue Behavior of an Ultrafine-Grained Al-Mg-Si Alloy Processed by High-Pressure Torsion"; Metals; 5(2); 2015.

[27] Feng L., Qian X.; "Low cycle fatigue test and enhanced lifetime estimation of high-strength steel S550 under different strain ratios"; Marine Structures; 61; 2018; 343–360.

[28] Garbatov Y., Guedes-Soares C., Parunov J,; "Fatigue strength experiments of corroded small scale steel specimens"; International Journal of Fatigue; 59; 2014; 137-144.

[29] ASTM E647-15; Standard Test Methods for Measurement of Fatigue Crack Growth Rates; ASTM International; West Conshohocken, PA; 2015.

[30] Anderson T.L.; "Fracture Mechanics, Fundamentals and Applications", 3rd ed., CRC Press, Taylor & Francis Group, 2005, 410-423.

[31] Escalero M., Blasón S., Zabala H., Torca I., Urresti I., Muniz-Calvente M., Fernández-Canteli A.; "Study of alternatives and experimental validation for predictions of hole-edge fatigue crack growth in 42CrMo4 steel"; Engineering structures 176; 2018; 621-631.

[32] Ebara R., "Corrosion fatigue crack initiation in 12% chromium stainless Steel", Materials Science and Engineering A 468-470, 2007, 109-113

[33] Gruenberg K.M., Craig B.A., Hillberry B.M., Bucci R.J., Hinkle A.J.; "Predicting fatigue life of pre-corroded 2024-T3 aluminum"; International Journal of Fatigue 26; 2004;: 629-640.

[34] Evans, C., Leiva-Garcia R., Akid R.; "Strain evolution around corrosion pits under fatigue loading"; Theoretical and Applied Fracture Mechanics 95; 2018; 253–260

[35] Sander M.; "Sicherheit und Betriebsfestigkeit von Maschinen und Anlagen", Springer Vieweg, 2018.

[36] Lebahn J., Sander M.; "Determination of statistical secured residual lifetime based on sensitivity analysis and stochastic crack propagation simulation", 13th International Conference on Fracture, 2013.

[37] DuQuesnay D.L., Underhill P.R., Britt H.J.; "Fatigue crack growth from corrosion damage in 7075-T6511 aluminium alloy under aircraft loading"; Int J Fatigue 25; 2003; 371–377.

[38] Cerit M., Genel K., Eksi S.; "Numerical investigation on stress concentration of corrosion pit"; Engineering Failure Analysis 16; 2009; 2467–2472.

420